Recent Advances in Analysis and Design of Axial Flux Permanent Magnet Electric Machines

FNU Nishanth*, *Student Member, IEEE*, Joachim Van Verdeghem†, *Member, IEEE*, and Eric L. Severson*, *Member, IEEE*
*Department of Electrical and Computer Engineering, University of Wisconsin-Madison, Madison, WI 53706 USA
†Department of Mechatronic, Electrical Energy, and Dynamic Systems, Université catholique de Louvain, Belgium
{nishanth, eric.severson}@wisc.edu

***Abstract*—Axial flux permanent magnet machines (AFPM) are popular for applications that benefit from high torque density and an axially compact form factor, such as in-wheel traction drives. Although the radial flux permanent magnet machine (RFPM) and the AFPM work based on the same underlying principle, the differences in their geometry introduce complexities in analysis of the AFPM. In this paper, the different AFPM design variants, their sizing approaches, computationally efficient design optimization techniques, and manufacturing techniques reported in literature are reviewed. In addition to classical AFPM machines, emerging variants and research opportunities with potential to push the boundaries of electric machine technology are reviewed. These include bearingless AFPMs, magnetically geared AFPMs, and combined radial-axial flux machines.**

***Index Terms*—Axial flux machines, sizing, analysis, optimization, fabrication, bearingless machines, combined radial-axial flux machines, magnetically geared machines.**

I. Introduction

Axial flux machines are a compelling alternative to conventional radial flux machines, particularly for applications that demand high torque densities and a short axial length relative to the outer diameter [1], [2]. These machines are characterized by an axial flux path between the rotor and the stator. Several axial flux machine variants have been reported in literature. Although the axial flux PM machines (AFPM) are the most popular, variants such as axial flux induction and reluctance machines have also been studied e.g.: [3]–[5]. Owing to the popularity of the AFPM compared to the other axial flux machines, the analysis presented in this paper focuses on the AFPM, but can be extended to other variants.

While AFPM have been previously reviewed in [2], [6], there has since been considerable advancement in the state of the art. For instance, new techniques have been developed for design optimization of AFPM e.g.: [7], [8]. Innovation in additive manufacturing of metals has opened avenues to manufacture electric machine geometries that are otherwise difficult to fabricate with conventional techniques [9], [10]. In addition, recent advancements such as bearingless and magnetically geared AFPM that combine the advantages of magnetic levitation and magnetic gears have positioned the AFPM technology to make a disruptive impact in the future of electric motor systems.

This material is based upon work supported by the U.S. Department of Energy Office of Energy Efficiency and Renewable Energy (EERE) under the Award Number DE-EE0008384.

The main contribution of this paper is to provide a review of the state of the art in AFPM machines. This paper is organized into four main parts. The first part reviews analytical techniques to size the AFPM. These techniques are used to identify application scenarios where AFPM can outperform RFPM. In the second part of this paper, design evaluation and optimization techniques for AFPMs are reviewed. These techniques are useful to efficiently evaluate candidate designs and explore the design space. The third part of this paper reviews the materials and manufacturing techniques reported in literature to fabricate axial flux machines. The relative merits of each of these techniques are identified. The final part of this paper concludes by reviewing the emerging AFPM topologies, providing a research outlook for the AFPM technology, and identifying promising avenues for future development.

II. AFPM Analysis

Several axial flux machine design variants have been reported in literature. This section reviews the different AFPM analysis and design techniques. The physical significance of the AFPM design parameters are highlighted, and a torque dense AFPM design is compared with the RFPM. A comprehensive classification of the AFPM design variants presented in [2] is shown in Fig. 1a. Among the design variants presented in Fig. 1a, the single sided and the torus type machines are popular for power dense applications. The torus type includes popular AFPM variants, such as the coreless machine, yokeless and segmented armature (YASA) machine, as well as the toroidal winding machine. More information about these variants can be found in [11], [12].

A. Sizing equations

Electric machine sizing equations relate the output of the machine to the design parameters of electric loading $\hat{A}$, magnetic loading $\hat{B}_\delta$, and the machine dimensions. In this section, the sizing equations for the axial and radial flux machines are presented. The physical significance of $\hat{A}$ and $\hat{B}_\delta$, and the nuances in their definition for AFPMs are highlighted.

1) Electric loading: In electric machine design, it is a well-accepted practice to define an equivalent linear current density on the stator surface that emulates the same fields as the physical slot currents. The fundamental component of this current density is responsible for producing the average

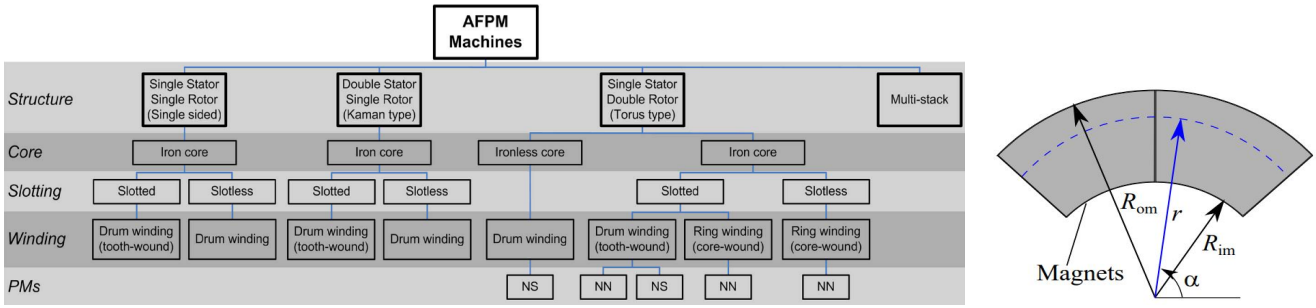

(a) (b)

Fig. 1. (a) Classification of AFPM topologies [2]; (b) Main radial dimensions of an AFPM [11].

electromagnetic torque and can be calculated as (1), where α is the angular location in the airgap, p is the number of pole-pairs, $z_Q\hat{I}$ is the number of ampere turns in a coil side, $k_{w,1}$ is the fundamental winding factor, N is the number of coils per phase, and r is the radius of the current location [13]. The peak value $\hat{A}$ of the linear current density is called the electric loading. The electric loading is a fundamental design parameter that is determined by the physical currents flowing in the stator slots. The maximum achievable electric loading is determined by the thermal considerations for a given design. The typical values of $\hat{A}$ for RFPM designs can be chosen based on the experience of the designer or using standard tables from literature, such as [13], [14].

$$A(\alpha) = \hat{A}\sin(p\alpha - \alpha_w), \quad \hat{A} = \left(\frac{3k_{w,1}z_Q\hat{I}N}{\pi r}\right) \tag{1}$$

2) Magnetic loading: The magnetic loading $\hat{B}_\delta$ is defined as the peak of the magnetizing (or no-load) airgap field fundamental component–see (2). In PM machines, the magnetic loading is created by the permanent magnets and is limited by the saturation limits and core-loss in the electrical steel. The magnetic loading $\hat{B}_\delta$ can be related to the permanent magnet thickness and airgap length in a similar manner for both RFPM and AFPM machines.

$$B_\delta(\alpha) = \hat{B}_\delta\cos(p\alpha - \theta) \tag{2}$$

3) Electric machine sizing: The Maxwell stress tensor can be used to integrate the airgap field quantities produced by the electric and magnetic loading to calculate the electromagnetic torque of electric machines, as presented in [13]. This results in the sizing equation (3) for radial flux PM machines. Here, T is the electromagnetic torque, R_o is the airgap radius and L is the axial length.

$$T = \pi R_o^2 L\hat{B}_\delta\hat{A} \tag{3}$$

Unlike the RFPM, a single airgap radius cannot be defined for an AFPM. As shown in Fig. 1b, the airgap spans from the inner radius R_{im} through the outer radius R_{om}. This presents nuances in identifying an appropriate radius r to define the electric loading per equation (1) for an AFPM. Two approaches to size the AFPM are popular in literature. The first approach proposed by Huang *et al.* in [1] relates the mechanical power P_{mech} to the machine dimensions using (4),

$$P_{mech} = C_{mech}fD_{om}^2L_e \tag{4}$$

where f is the fundamental frequency and $C_{mech} = \frac{\pi}{2}K_eK_iK_LK_p\eta\hat{B}_\delta\hat{A}_{avg}\frac{1}{p}\frac{((1-\lambda^2)(1+\lambda)}{2}$ is the Essen's coefficient, $D_{om} = 2R_{om}$ is the outer diameter of the machine, $\lambda = \frac{R_{im}}{R_{om}}$ is the radius ratio, and $L_e = R_{om} - R_{im}$ is the effective stack length. A discussion of each parameter in C_{mech} is provided in [1]. In this expression, the electric loading $\hat{A}_{avg}$ is defined at the average radius $\frac{R_{om}+R_{im}}{2}$. It is also shown that λ is the only independent term in this sizing equation and all other parameters either depend on λ or have a very limited range.

The other popular sizing approach is presented in [15], [16]. The electric loading in these expressions is defined at the inner radius R_{im}. However, as the airgap extends in the radial direction, the electric loading will not be uniform at all radii. Therefore, the electric loading $\hat{A}$ needs to be considered as a function of the radius $r \in [R_{im}, R_{om}]$ (Fig. 1b). A detailed derivation of the sizing equation, considering the electric loading as a function of the radius is presented in [11]. For the YASA, coreless, and single sided AFPM, this equation can be expressed in terms of the geometric ratio $\lambda = \frac{R_{im}}{R_{om}}$ as

$$T = \frac{\pi}{2}\hat{B}_\delta\hat{A}R_{om}^3\lambda(1-\lambda^2) \tag{5}$$

It is seen that the electromagnetic torque of the AFPM varies as the cube of its outer radius and the geometric ratio λ is again an important design parameter. The range $\lambda \in [0.65, 0.75]$ has been reported for power dense designs in [2].

B. Comparison of design variants

Several comparisons of AFPM and RFPM designs have been reported in literature. The power density of toroidal AFPM, two stator AFPM, and RFPM designs was compared in [1] using the generalized sizing equation (4). It was shown that both the AFPM design variants compared were more power dense than the RFPM. Taran *et al.* in [17], [18] and Nishanth *et al.* in [11] showed that the YASA and the single-sided AFPM have the same torque capability when the same PM volume is used. This implies approximately twice the torque per rotor volume, and lower active material cost for the single-sided AFPM.

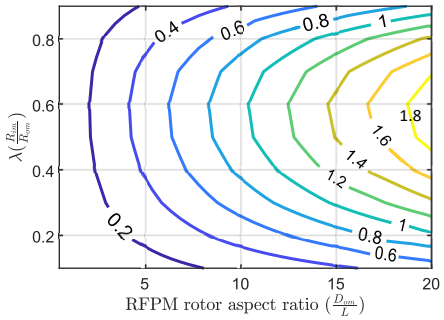

Fig. 2. Comparison of AFPM and RFPM torque capability

The sizing equations can be used to compare the torque capability of single rotor-single stator AFPM and RFPM designs for different aspect ratios of the RFPM rotor. Using (3) and (5), the following equation can be derived:

$$\frac{T_{\text{afpm}}}{T_{\text{rfpm}}} = \frac{\frac{\pi}{2}\hat{B}_\delta \hat{A} R_{\text{om}}^3 \lambda(1-\lambda^2)}{\pi R_{\text{om}}^2 L \hat{B}_\delta \hat{A}} = \frac{D_{\text{om}}\lambda(1-\lambda^2)}{4L} \tag{6}$$

where $D_{\text{om}} = 2R_{\text{om}}$ is the outer diameter of the AFPM and RFPM rotors, and $\frac{D_{\text{om}}}{L}$ is the aspect ratio of the RFPM rotor.

Figure 2 compares the AFPM and RFPM designs using (6) for different values of λ. Each contour shows the torque ratio between AFPM and RFPM. At RFPM rotor aspect ratios less than 12, it can be seen that the AFPM with the same outer radius R_{om} produces lower torque. However, at RFPM rotor aspect ratios greater than 12, the AFPM with the same R_{om} can produce higher torque compared to the equivalent RFPM. This analysis assumes that the same value of electric loading is achievable in the AFPM and RFPM. In reality, the AFPM structure is more conducive to cooling [17] compared to the RFPM. This makes higher electric loading achievable and can further improve the AFPM torque capability.

The torque per rotor volume (TRV) can also be used to compare RFPM and AFPM designs. From (3), the TRV for RFPM designs is given by $\text{TRV}_{\text{rfpm}} = \hat{B}_\delta \hat{A}$, and the TRV for AFPM can be computed as $\text{TRV}_{\text{afpm}} = \frac{\lambda R_{\text{om}}}{2(t_{\text{m}}+t_{\text{y}})}\hat{B}_\delta \hat{A}$. For most practical designs, the combined thickness of the PM and rotor yoke are such that $t_{\text{m}} + t_{\text{y}} < \frac{\lambda R_{\text{om}}}{2}$, resulting in a higher TRV for AFPM compared to an equivalent RFPM.

III. Analysis and Design Optimization

Electric machine designs have several variables that affect the design objectives. To identify designs that satisfactorily meet all design objectives, a design optimization study that couples electric machine analysis with an optimization algorithm is essential [19]. The flux paths in AFPM are three dimensional. In addition, there are two major 3D effects that occur in the AFPM [2]: i) radial dependency of the flux distribution due to variation in the slot, tooth, and pole dimensions in the radial direction, and ii) flux fringing at the inner and outer radii. Accurate performance analysis of AFPM designs requires taking these 3D effects into consideration. This has led to development of analytic and semi-analytic techniques that trade-off evaluation time for accuracy. Promising analytic techniques e.g.: [20], [21], were comprehensively reviewed in [2]. Although the analytical techniques are computationally efficient, FEA is the most accurate technique to evaluate AFPM designs [2]. This makes an FEA-based design optimization desirable.

Two design optimization approaches are popular to overcome the large computational requirements of 3D FEA (most accurate for AFPM evaluation): i) Reducing the number of 3D FEA solves using numerical techniques, and ii) Using 2D FEA evaluation. The choice of the suitable approach for a given problem depends upon the AFPM design variant being analyzed and the accuracy required for the application.

1) Design optimization with reduced number of 3D solves: In this approach, only a few designs are evaluated using 3D FEA and the rest of the designs are evaluated using numerical techniques like surrogate models or artificial neural networks. A two-level surrogate-assisted optimization approach (2L-SAMODE) for AFPM was reported in [7]. In this method, kriging surrogate models are used to estimate performance parameters of the electric machine designs and 3D FEA is only used to evaluate pareto-optimal designs in each generation. The Pareto fronts obtained using the 2L-SAMODE and conventional multi-objective differential evolution (MODE) were approximately the same as seen from Fig. 3a. The MODE required 886 FEA evaluations while the 2L-SAMODE required only 163 FEA evaluations to generate the same Pareto front. This technique was also adopted in [23].

2) 2D FEA techniques: 2D FEA techniques for AFPM design evaluation have been reported in [22], [24]–[26]. These 2D FEA analysis techniques divide the AFPM into several 2D computation planes (Fig. 3b) and perform a series of FEA solves at each computation plane. A popular method is to consider each 2D computation plane as a linear machine as proposed in [24], [25]. Gulec *et al.* investigated three different approaches for 2D FEA analysis of AFPM in [22]. These approaches included considering the 2D computation planes as i) linear machine (LMMA), ii) inner rotor machine (IRMA), and iii) outer rotor machine (ORMA) as shown in Fig. 3b. The LMMA approach was found to have the least computation time. The performance parameters computed with 2D FEA were in closer agreement with experimental values for coreless designs compared to iron cored designs. This was attributed to the non-linearity of iron (absent in the coreless design).

Performance parameters computed using 3D FEA and 2D FEA using the LMMA approach with 3 computation planes were compared in [25] for a coreless AFPM design rated for 20 kW and 15,000 RPM. It was shown that the 2D FEA significantly reduced computation time, with marginal reduction in accuracy, making it suitable for design optimization.

IV. Materials and Manufacturing

One of the reasons for lower commercial adoption of AFPMs is the difficulty in fabrication with conventional manufacturing techniques. This section reviews the recent trends in AFPM fabrication. The popular techniques reported in literature to manufacture the stator and the PM rotor are reviewed and their relative merits highlighted.

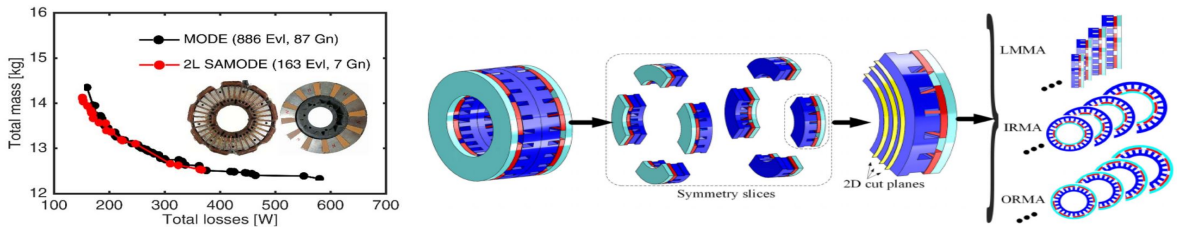

(a) (b)

Fig. 3. (a) Comparison of Pareto fronts obtained using MODE and two level surrogate assisted MODE [7] for a commercial AFPM. Evl indicates the number of 3D FEA evaluations to reach the Pareto front.; (b) Schematic showing 2D modeling approaches for AFPM [22]

A. Stator design

The stator structure can significantly vary between AFPM design variants. They can be iron cored, coreless, or yokeless with segmented armature (YASA). Electric machine stator cores are nearly always fabricated using laminated electrical steel to reduce eddy current losses. Unlike RFPMs, where laminations can be axially stacked, AFPMs require radial laminations, which are difficult to assemble. Several manufacturing approaches for AFPM stators are now summarized.

1) Laminated steel: Tape-wound cores built using thin gauge electrical steel have been used to fabricate toroidal slotless AFPM stators, e.g.: [27], [28]. This is a popular and relatively simple approach that does not require specialized manufacturing techniques or equipment. Slots can be cut into the tapewound cores to fabricate slotted stator AFPM variants. Sahin used wire EDM technique in [29] to cut slots into a tapewound core for a 30kW, 16,000 RPM axial flux generator (Fig. 4a). A similar approach was adopted in [30], where the slots were machined instead. It was noted that the machining process to create slots can introduce short circuits between the lamination layers. Another variant is to wind stamped steel tape as shown in Fig. 4b [31]. This requires specialized equipment and is relatively expensive.

2) Soft magnetic composites: Soft magnetic composites (SMC) have been reported in literature such as [31]–[34] for AFPM stator fabrication. This method can have high initial cost for the SMC molds compared to using laminated steel. In [34], Kim *et al.* compared the performance of SMC and laminated stator cores for the 14-pole, 12-slot AFPM shown in Fig. 4c. The results are shown in Fig. 4d. It can be seen that the laminated core was more efficient at low operating speeds (lower frequency). However, at higher operating frequencies the SMC and the laminated cores had comparable efficiencies. This was attributed to the increased eddy current losses in the laminated steel at higher operating frequencies.

3) PCB stator: PCB stators have been studied and used for AFPM designs, e.g. [23], [35]–[38], and comprehensively reviewed in [39]. A PCB stator with rhomboidal windings is presented in [35] for a miniature spindle motor shown in Fig. 4e. It was shown in [36] that the trapezoidal winding better utilizes the board area and has a higher torque producing capability than the rhomboidal pattern. Wave winding schemes for PCB stators were compared in [37] and the non-overlapping radial wave winding was identified to have the highest fundamental back-EMF and torque capability. The performance of a laminated stator and a PCB stator was compared in [38]. For the same output power, the machine with the PCB stator was more efficient and compact. However, the PCB stator had significant thermal limitations on achieving higher current densities. It can be concluded that, although the PCB windings are promising for low voltage and current ratings, with the current state of the art, there will be challenges in using it successfully at elevated voltages and current densities.

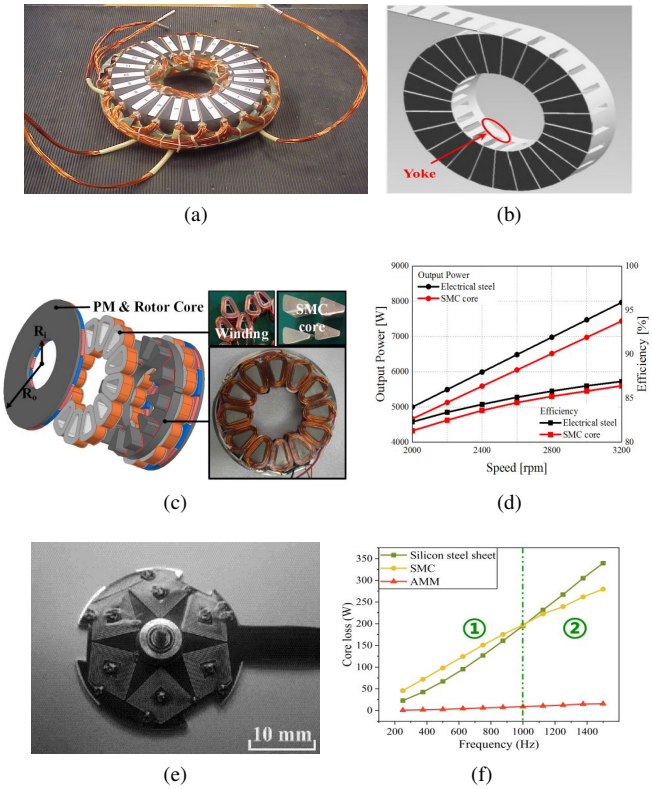

(a) (b) (c) (d) (e) (f)

Fig. 4. AFPM stator examples: (a) Tapewound core with slots cut using EDM [29]; (b) Slotted stator using stamped lamination [31]; (c) AFPM using SMC core [34]; (d) Efficiency comparison between SMC and laminated stator [34]; (e) PCB windings [35]; (f) Core loss v/s frequency for laminated, SMC, and additively manufactured (AMM) stators [31];

4) Additive manufacturing: Additive manufacturing techniques are currently being investigated for AFPMs e.g. [40], [41]. Sun *et al.* compared laminated, SMC, and additively manufactured stators for a multi-stage AFPM in [31]. It was noted that the core losses for the additively manufactured stator

were lower than the laminated and SMC stators in both the low and high frequency (over 1kHz) operating regions, as shown in Fig. 4f. In addition to stator core, additive manufacturing techniques can also be used to fabricate the windings.

B. Rotor design

The AFPM rotors typically require non-standard shapes of PM, which can be expensive. However, high performance rotors have been adapted in literature to use conventional-shaped PMs and reduce cost, e.g. [42], [44]. In addition to being cost effective, having smaller PM segments per pole, also reduces losses due to induced eddy currents. Vansompel *et al.* compared a T-shaped pole structure with different number of magnet segments per pole for a 4 kW, 2,500 RPM YASA machine in [42]. The final pole structure shown in Fig. 5a has 14 cuboidal NdFeB segments per pole which reduced the eddy current losses by a factor of 8 compared to unsegmented poles. A coreless AFPM with circular pole shapes as shown in Fig. 5c was developed in [44].

Halbach array rotors for AFPM have been reported in [43], [46]–[49]. These rotors are frequently used for ironless stator AFPM primarily due to the inherent sinusoidal air-gap field distribution and flux focusing capability [46]. Zhang *et al.* in [46] reported a detailed mechanical design of a Halbach array rotor for a 50 kW coreless AFPM. The prototype reached speeds of up to 9000 RPM while remaining mechanically stable. A quasi-Halbach array rotor shown in Fig. 5b was reported to provide a 12% increase in torque density of a torus machine compared to an axially magnetized PM array in [43].

PM shapes can also be used as a design handle to improve the machine performance. The effect of PM shape on AFPM performance has been analyzed in [45], [50]–[52]. Different cost-effective PM skewing techniques shown in Fig. 5d were reviewed in [45] to reduce cogging torque of double rotor AFPM machines. It was found that triangular skew significantly reduced the cogging torque compared to the unskewed design, and offered performance similar to the classic skew. In [50], an interior permanent magnet (IPM) rotor design with sinusoidal shaped magnets was proposed for a coreless AFPM. This design was 35% more torque dense and had 60% lower THD compared to a reference conventional coreless AFPM. To reduce the cogging torque, [51] compared the following PM arrangements i) a pole arc ratio of 0.81, ii) alternating pole arc ratios of 0.61 and 0.81, and iii) skew by one pole pitch. Compared to a 0.81 pole arc rotor, alternating pole arcs effectively reduced cogging torque by 73%, whereas the skewed poles reduced the cogging torque by 48%.

V. Emerging topologies and Research Outlook

Recently, new AFPM topologies such as bearingless AFPM, magnetically geared AFPM, and combined radial and axial flux machines have garnered significant research interest. These new topologies are now reviewed and opportunities are identified for further research in AFPM technology to disrupt the state of electric machinery.

A. Bearingless AFPM

Bearingless machines integrate motor and magnetic suspension capabilities within a single structure. This integration combines the advantages of AFPM motors and those of levitation, namely no mechanical wear, no lubrication, and higher speed range, while still offering torque dense designs. Applications of these motors encompass centrifugal pumps, ventricular assist devices and artificial hearts, reaction wheels as well as flywheels [53]. These motors traditionally comprise separate coils for the motor and magnetic levitation, creating a trade-off in the winding space allocation. Gathering both of these functions within a combined winding (same coils used for motor and levitation) increases the torque density given that almost the entire slot space can be used for torque production during normal operation and for the suspension in emergency conditions [54]. Furthermore, double-sided structures are typically preferred as their axial symmetry allows the unstable attraction forces acting between the stator and the rotor in the centered position to compensate for each other [55].

Bearingless machines can be classified based on the number of rotor degrees of freedom (DOF) being actively regulated. Most examples of AFPM bearingless motors actively regulate axial forces (1-DOF) in addition to the motor torque, while the tilt and radial motions are stabilized with passive permanent magnet bearings or through reluctance forces. Various topologies of one-axis controlled machines have been proposed. They include double-sided slotted armature with non-salient [55], [56] and salient rotor [57] but also single-sided slotted [58] and coreless designs [59], [60]. Among them, several structures rely on a combined armature winding supplied by a single three-phase inverter to generate both the axial force and the torque [56], [58]–[60]. These so-called single-drive motors are therefore more compact, more energy-efficient and less expensive than classic one-axis bearingless machines.

Literature reports 2-DOF Lorentz-type bearingless motors that actively regulate the radial forces [61]–[63]. Their ironless stator structure eliminates slot harmonics as well as stator iron losses. In addition, no negative stiffness is created in the axial and tilt directions, preventing the underlying static instability. A 3-DOF single-sided slotted bearingless machine has also been proposed in [64] and further investigated in [65], [66]. The axial and tilt motions are regulated through currents supplied to a combined winding whereas passive reluctant forces provide radial stabilization, leading to a compact implementation. Additionally, axial-flux motors designed to actively regulate 5-DOF have been investigated. Each stator of these double-sided machines is constituted of either a single winding [67], [68] or two separate windings, one handling the axial force and drive torque production and the other one the radial and tilt forces [69]–[71].

Recent research introduced fully passively levitated bearingless machines based on an electrodynamic thrust bearing with additional coils for the torque creation [72]. This concept was further improved by integrating both motor function and passive axial levitation within a combined winding [73], [74].

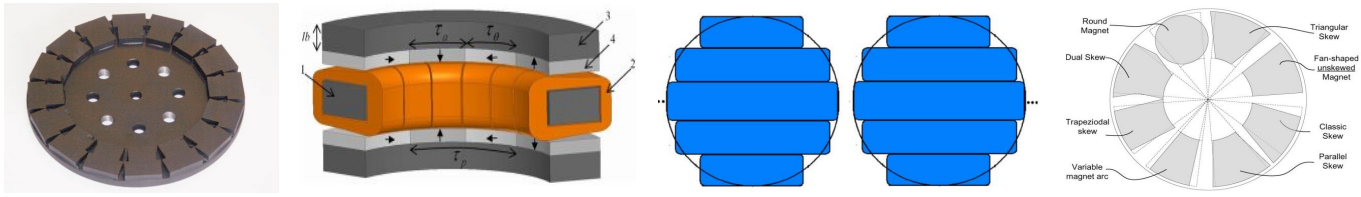

(a) (b) (c) (d)

Fig. 5. (a) T-shaped PM with 14 cuboidal segments per pole [42]; (b) Torus machine with quasi-Halbach rotor [43]. The parts are 1 - stator core, 2 - toroidal winding, 3 - rotor core, and 4 - quasi Halbach array; (c) Circular pole shape using rectangular PM [44]; (d) Rotor skew techniques for AFPM [45]

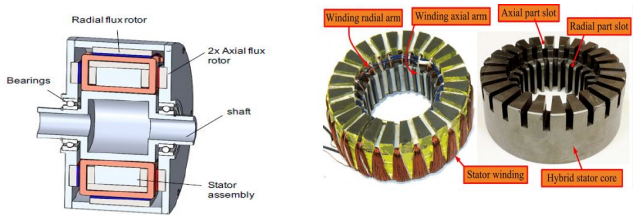

(a) (b)

Fig. 6. Combined flux machines: (a) Cross-section of a combined flux PM vernier machine [78]; (b) Combined flux hysterisis machine stator [79].

The axial force production is achieved through electrodynamic phenomena resulting from currents induced in the windings. These machines can be operated by a three-phase inverter without any additional position sensor, power electronics or controller with respect to a conventional motor. The reliability and compactness are thus improved and the cost is reduced.

B. Combined radial-axial flux machines

The end-windings of conventional electric machines do not contribute to the torque. The end-windings of RFPM require an axial flux path, while the end-windings of AFPM require a radial flux path for useful torque production. Combined radial-axial flux electric machine topologies are now being developed, e.g. as [75]–[79]. These machines use both the radial and axial flux paths for torque production, thereby improving the torque density. However, these machines are challenging to fabricate with the conventional AFPM and RFPM lamination techniques.

Jack *et al.* in [75] built and tested a combined radial-axial flux PM machine with an SMC stator. Zhou *et al.* in [78] built a combined radial-axial flux PM vernier machine shown in Fig. 6a for a low-speed high-torque direct-drive application. This machine showed potential to generate 1.5 times the torque of the baseline machine that it replaced. Nasiri-Zarandi *et al.* built a combined radial-axial flux hysterisis machine in [79] using soft magnetic ferrite (Mn–Zn) for the stator core. Compared to axial flux machine of the same form factor, the combined machine reported a 40% higher torque capability.

C. Magnetically geared AFPM

Magnetically geared machines integrate the capabilities of a magnetic gear with that of an electric machine. This can result in a significant increase in torque density and multiple rotating shafts at different speeds, making this technology attractive for direct-drive and vehicle electrification applications [80], [81].

Magnetically geared axial flux machines are a new and active research space, e.g. [8], [82], [83]. A magnetically geared axial flux generator with a torque density of 7.8 kNm/m^3 was prototyped in [84] and simulation results showed that designs rated at up to 60 kNm/m^3 are realizable. Khatab *et al.* compared the performance of magnetically geared and conventional YASA machines in [85]. For the same machine volume and axial length, it was shown that the magnetically geared YASA machine achieves approximately twice the torque density of the conventional YASA machine.

D. Research outlook

All users of electric machines desire optimal power density, efficiency, reliability, lifetime, and cost. Research opportunity exists to alter the limits of electric machine technology in these areas by leveraging the advancements in AFPM machines reviewed in Sections III and IV in the three emerging technology variants reviewed in this section. Magnetic levitation can improve reliability, lifetime, and efficiency while enabling higher operating speeds to increase power density. The magnetically geared and the combined radial and axial flux machines show promise to significantly improve power density and cost per kW by pushing the limits of achievable torque density.

The literature reviewed in this paper reports proof of concept for these emerging technologies, but high performance and practical demonstrations at significant power scales have not yet been reported. To realize their disruptive potential, all three of the emerging variants require optimization of challenging 3D models and innovative, low-cost manufacturing techniques. Future research is needed to navigate the trade-off between torque density and force vector error and minimize drive cost in bearingless machines; enable higher rotational speeds and improve the power factor for magnetically geared machines; and develop practical and affordable geometry for efficient combined radial-axial machines.

VI. Conclusion

This paper presented a review of the state of the art in modeling, analysis, and manufacturing of axial flux PM machines. Emerging electric machine topologies that have recently garnered significant research interest were also reviewed, and a research outlook was presented. The analysis, optimization, and manufacturing techniques reviewed in this paper, along with the recent advances in manufacturing techniques such as use of improved SMCs and additive manufacturing of metals, have the potential to enable wide commercial adoption of AFPM machines. The paper further finds that if AFPM machines integrate features of magnetic levitation and magnetic gears,

they can push the boundaries of reliability, rated speed, specific torque, and power density for electric machine technology.

REFERENCES

[1] S. Huang, J. Luo, F. Leonardi, and T. A. Lipo, "A comparison of power density for axial flux machines based on general purpose sizing equations," *IEEE Transactions on Energy Conversion*, vol. 14, no. 2, pp. 185–192, Jun. 1999.

[2] F. G. Capponi, G. D. Donato, and F. Caricchi, "Recent Advances in Axial-Flux Permanent-Magnet Machine Technology," *IEEE Transactions on Industry Applications*, vol. 48, no. 6, pp. 2190–2205, 2012.

[3] J. Mei, C. Lee, and J. L. Kirtley, "Design of Axial Flux Induction Motor With Reduced Back Iron for Electric Vehicles," *IEEE Transactions on Vehicular Technology*, vol. 69, no. 1, pp. 293–301, Jan. 2020.

[4] B. Dianati, S. Kahourzade, and A. Mahmoudi, "Optimization of axial-flux induction motors for the application of electric vehicles considering driving cycles," *IEEE Transactions on Energy Conversion*, vol. 35, no. 3, pp. 1522–1533, 2020.

[5] W. Sun, Q. Li, L. Sun, L. Zhu, and L. Li, "Electromagnetic Analysis on Novel Rotor-Segmented Axial-Field SRM Based on Dynamic Magnetic Equivalent Circuit," *IEEE Transactions on Magnetics*, vol. 55, no. 6, pp. 1–5, Jun. 2019.

[6] S. Kahourzade, A. Mahmoudi, H. W. Ping, and M. N. Uddin, "A Comprehensive Review of Axial-Flux Permanent-Magnet Machines," *Canadian Journal of Electrical and Computer Engineering*, vol. 37, no. 1, pp. 19–33, 2014.

[7] N. Taran, D. M. Ionel, and D. G. Dorrell, "Two-level surrogate-assisted differential evolution multi-objective optimization of electric machines using 3-d fea," *IEEE Transactions on Magnetics*, vol. 54, no. 11, pp. 1–5, 2018.

[8] Q. Wang, F. Zhao, and K. Yang, "Analysis and optimization of the axial electromagnetic force for an axial-flux pm vernier machine," *IEEE Transactions on Magnetics*, vol. 57, no. 2, pp. 1–5, 2021.

[9] R. Wrobel and B. Mecrow, "A comprehensive review of additive manufacturing in construction of electrical machines," *IEEE Transactions on Energy Conversion*, vol. 35, no. 2, pp. 1054–1064, 2020.

[10] M. U. Naseer, A. Kallaste, B. Asad, T. Vaimann, and A. Rassõlkin, "A review on additive manufacturing possibilities for electrical machines," *Energies*, vol. 14, no. 7, pp. 1940–1964, 2021.

[11] F. Nishanth, G. Bohach, M. M. Nahin, J. Van de Ven, and E. L. Severson, "Design of an axial flux machine with an integrated hydraulic pump for off-highway vehicle electrification," in *2020 IEEE Energy Conversion Congress and Exposition (ECCE)*, 2020, pp. 1772–1779.

[12] T. Woolmer and M. McCulloch, "Analysis of the yokeless and segmented armature machine," in *2007 IEEE International Electric Machines Drives Conference*, vol. 1, 2007, pp. 704–708.

[13] J. Pyrhonen, T. Jokinen, and V. Hrabovcova, *Design of rotating electrical machines*. John Wiley & Sons, 2013.

[14] T. Lipo, *Introduction to AC machine design*. John Wiley & Sons, 2017.

[15] J. F. Gieras, R.-J. Wang, and M. J. Kamper, *Axial flux permanent magnet brushless machines*. Springer Science & Business Media, 2008.

[16] E. Spooner and B. Chalmers, ""TORUS": A slotless, toroidal-stator, permanent-magnet generator," in *IEE Proceedings B (Electric Power Applications)*, vol. 139, no. 6. IET, 1992, pp. 497–506.

[17] N. Taran, G. Heins, V. Rallabandi, D. Patterson, and D. M. Ionel, "Evaluating the effects of electric and magnetic loading on the performance of single- and double-rotor axial-flux pm machines," *IEEE Transactions on Industry Applications*, vol. 56, no. 4, pp. 3488–3497, 2020.

[18] ——, "Torque production capability of axial flux machines with single and double rotor configurations," in *2018 IEEE Energy Conversion Congress and Exposition (ECCE)*, 2018, pp. 7336–7341.

[19] G. Bramerdorfer, J. A. Tapia, J. J. Pyrhönen, and A. Cavagnino, "Modern electrical machine design optimization: Techniques, trends, and best practices," *IEEE Transactions on Industrial Electronics*, vol. 65, no. 10, pp. 7672–7684, 2018.

[20] Y. Zhilichev, "Three-dimensional analytic model of permanent magnet axial flux machine," *IEEE Transactions on Magnetics*, vol. 34, no. 6, pp. 3897–3901, 1998.

[21] O. de la Barriere, S. Hlioui, H. Ben Ahmed, M. Gabsi, and M. LoBue, "3-d formal resolution of maxwell equations for the computation of the no-load flux in an axial flux permanent-magnet synchronous machine," *IEEE Transactions on Magnetics*, vol. 48, no. 1, pp. 128–136, 2012.

[22] M. Gulec and M. Aydin, "Implementation of different 2d finite element modelling approaches in axial flux permanent magnet disc machines," *IET Electric Power Applications*, vol. 12, no. 2, pp. 195–202, 2018.

[23] M. G. Kesgin, P. Han, N. Taran, D. Lawhorn, D. Lewis, and D. M. Ionel, "Design optimization of coreless axial-flux pm machines with litz wire and pcb stator windings," in *2020 IEEE Energy Conversion Congress and Exposition (ECCE)*, 2020, pp. 22–26.

[24] A. Parviainen, M. Niemela, and J. Pyrhonen, "Modeling of axial flux permanent-magnet machines," *IEEE Transactions on Industry Applications*, vol. 40, no. 5, pp. 1333–1340, 2004.

[25] F. Nishanth, G. Bohach, J. V. de Ven, and E. L. Severson, "Design of a highly integrated electric-hydraulic machine for electrifying off-highway vehicles," in *2019 IEEE Energy Conversion Congress and Exposition (ECCE)*, 2019, pp. 3983–3990.

[26] X. Yang, D. Patterson, and J. Hudgins, "Design optimization of single-sided axial flux permanent magnet machines by differential evolution," in *International Conference on Electrical Machines*, 2014, pp. 1–5.

[27] M. Liben and D. C. Ludois, "Analytical design and experimental testing of a self-cooled, toroidally wound ring motor with integrated propeller for electric rotorcraft," *IEEE Transactions on Industry Applications*, vol. 57, no. 3, pp. 2342–2353, 2021.

[28] A. Ghaheri, A. Mohammadi Ajamloo, H. Torkaman, and E. Afjei, "Design, modelling and optimisation of a slot-less axial flux permanent magnet generator for direct-drive wind turbine application," *IET Electric Power Applications*, vol. 14, no. 8, pp. 1327–1338, 2020.

[29] F. Sahin, *Design and development of a high-speed axial-flux permanent-magnet machine*. T.U. Eindhoven, 2001.

[30] Q. A. Shah Syed, V. Solovieva, and I. Hahn, "Magnetization characteristics and loss measurements of the axial flux permanent magnet motor's stator," in *2019 IEEE International Electric Machines Drives Conference (IEMDC)*, 2019, pp. 1061–1066.

[31] S. Sun, F. Jiang, T. Li, B. Xu, and K. Yang, "Comparison of a multi-stage axial flux permanent magnet machine with different stator core materials," *IEEE Transactions on Applied Superconductivity*, vol. 30, no. 4, pp. 1–6, 2020.

[32] Y. Wang, J. Lu, C. Liu, G. Lei, Y. Guo, and J. Zhu, "Development of a High-Performance Axial Flux PM Machine With SMC Cores for Electric Vehicle Application," *IEEE Transactions on Magnetics*, vol. 55, no. 7, pp. 1–4, Jul. 2019.

[33] Z. Wang, R. Masaki, S. Morinaga, Y. Enomoto, H. Itabashi, M. Ito, and S. Tanigawa, "Development of an axial gap motor with amorphous metal cores," *IEEE Transactions on Industry Applications*, vol. 47, no. 3, pp. 1293–1299, 2011.

[34] C.-W. Kim, G.-H. Jang, J.-M. Kim, J.-H. Ahn, C.-H. Baek, and J.-Y. Choi, "Comparison of axial flux permanent magnet synchronous machines with electrical steel core and soft magnetic composite core," *IEEE Transactions on Magnetics*, vol. 53, no. 11, pp. 1–4, 2017.

[35] M.Tsai and L.Hsu, "Design of a miniature axial-flux spindle motor with rhomboidal pcb winding," *IEEE Transactions on Magnetics*, vol. 42, no. 10, pp. 3488–3490, 2006.

[36] M. D. Noh, J. Kim, and Y.-W. Park, "Comparisons of concentrated printed-circuit stator windings for axial flux permanent magnet machines," in *2019 IEEE/ASME International Conference on Advanced Intelligent Mechatronics (AIM)*, 2019, pp. 229–234.

[37] S. Paul, M. Farshadnia, A. Pouramin, J. Fletcher, and J. Chang, "Comparative analysis of wave winding topologies and performance characteristics in ultra-thin printed circuit board axial-flux pm machine," *IET Electric Power Applications*, vol. 13, no. 5, pp. 694–701, 2019.

[38] S. Neethu, S. P. Nikam, S. Pal, A. K. Wankhede, and B. G. Fernandes, "Performance comparison between pcb-stator and laminated-core-stator-based designs of axial flux permanent magnet motors for high-speed low-power applications," *IEEE Transactions on Industrial Electronics*, vol. 67, no. 7, pp. 5269–5277, 2020.

[39] O. Taqavi and S. M. Mirimani, "Design aspects, winding arrangements and applications of printed circuit board motors: comprehensive review," *IET Electric Power Applications*, vol. 14, no. 9, pp. 1505–1518, 2020.

[40] M. Bonnet, Y. Lefevre, J. Llibre, D. Harribey, F. Defay, and N. Sadowski, "3d magnetic field model of a permanent magnet ironless axial flux motor with additively manufactured non-active parts," in *19th International Symposium on Electromagnetic Fields (ISEF)*, 2019, pp. 1–2.

[41] H. Tiismus, A. Kallaste, T. Vaimann, A. Rassõlkin, and A. Belahcen, "Additive manufacturing of prototype axial flux switched reluctance machine," in *International Workshop on Electric Drives*, 2021, pp. 1–4.

[42] H. Vansompel, P. Sergeant, and L. Dupré, "Effect of segmentation on eddy-current loss in permanent-magnets of axial-flux pm machines using a multilayer-2d — 2d coupled model," in *XXth International Conference on Electrical Machines*, 2012, pp. 228–232.

[43] I. P. Wiltuschnig, P. R. Eckert, D. G. Dorrell, and A. F. Flores Filho, "A study of the influence of quasi-halbach arrays on a torus machine," *IEEE Transactions on Magnetics*, vol. 52, no. 7, pp. 1–4, 2016.

[44] S. Javadi and M. Mirsalim, "A coreless axial-flux permanent-magnet generator for automotive applications," *IEEE Transactions on Magnetics*, vol. 44, no. 12, pp. 4591–4598, 2008.

[45] M. Aydin and M. Gulec, "Reduction of cogging torque in double-rotor axial-flux pm disk motors: A review of cost-effective magnet-skewing techniques with experimental verification," *IEEE Transactions on Industrial Electronics*, vol. 61, no. 9, pp. 5025–5034, 2014.

[46] Z. Zhang, C. Wang, and W. Geng, "Design and optimization of halbach-array pm rotor for high-speed axial-flux permanent magnet machine with ironless stator," *IEEE Transactions on Industrial Electronics*, vol. 67, no. 9, pp. 7269–7279, 2020.

[47] B. Zhang, T. Seidler, R. Dierken, and M. Doppelbauer, "Development of a Yokeless and Segmented Armature Axial Flux Machine," *IEEE Transactions on Industrial Electronics*, vol. 63, no. 4, pp. 1–10, 2016.

[48] W. Geng and Z. Zhang, "Analysis and Implementation of New Ironless Stator Axial-Flux Permanent Magnet Machine With Concentrated Nonoverlapping Windings," *IEEE Transactions on Energy Conversion*, vol. 33, no. 3, pp. 1274–1284, Sep. 2018.

[49] S. Neethu, S. P. Nikam, S. Singh, S. Pal, A. K. Wankhede, and B. G. Fernandes, "High-speed coreless axial-flux permanent-magnet motor with printed circuit board winding," *IEEE Transactions on Industry Applications*, vol. 55, no. 2, pp. 1954–1962, 2019.

[50] M. Aydin and M. Gulec, "A new coreless axial flux interior permanent magnet synchronous motor with sinusoidal rotor segments," *IEEE Transactions on Magnetics*, vol. 52, no. 7, pp. 1–4, 2016.

[51] J. Wanjiku, M. A. Khan, P. S. Barendse, and P. Pillay, "Influence of Slot Openings and Tooth Profile on Cogging Torque in Axial-Flux PM Machines," *IEEE Transactions on Industrial Electronics*, vol. 62, no. 12, pp. 7578–7589, Dec. 2015.

[52] M. Shokri, N. Rostami, V. Behjat, J. Pyrhönen, and M. Rostami, "Comparison of performance characteristics of axial-flux permanent-magnet synchronous machine with different magnet shapes," *IEEE Transactions on Magnetics*, vol. 51, no. 12, pp. 1–6, 2015.

[53] J. Chen, J. Zhu, and E. L. Severson, "Review of bearingless motor technology for significant power applications," *IEEE Transactions on Industry Applications*, vol. 56, no. 2, pp. 1377–1388, 2020.

[54] A. Khamitov, W. Gruber, G. Bramerdorfer, and E. L. Severson, "Comparison of combined winding strategies for radial non-salient bearingless machines," *IEEE Transactions on Industry Applications*, pp. 1–14, 2021.

[55] S. Ueno and Y. Okada, "Characteristics and control of a bidirectional axial gap combined motor-bearing," *IEEE/ASME Transactions on Mechatronics*, vol. 5, no. 3, pp. 310–318, 2000.

[56] J. Asama, Y. Hamasaki, T. Oiwa, and A. Chiba, "Proposal and analysis of a novel single-drive bearingless motor," *IEEE Transactions on Industrial Electronics*, vol. 60, no. 1, pp. 129–138, 2013.

[57] Q. D. Nguyen and S. Ueno, "Modeling and control of salient-pole permanent magnet axial-gap self-bearing motor," *IEEE/ASME Transactions on Mechatronics*, vol. 16, no. 3, pp. 518–526, 2011.

[58] S. Ueno and Y. Okada, "Characteristics of axial force and rotating torque and their control of permanent magnet type axial gap self-bearing motor," *Electrical Engineering Japan*, vol. 132, no. 1, pp. 81–91, 2000.

[59] J. Asama, D. Watanabe, T. Oiwa, and A. Chiba, "Development of a one-axis actively regulated bearingless motor with a repulsive type passive magnetic bearing," in *International Power Electronics Conference (IPEC-Hiroshima 2014)*, 2014, pp. 988–993.

[60] J. Van Verdeghem, E. L. Severson, and B. Dehez, "Hybrid active-passive actuation approach of passively levitated thrust self-bearing machines," *IEEE Transactions on Industry Applications*, pp. 1–12, 2021.

[61] Woo-Sup Han, Chong-Won Lee, and Y. Okada, "Design and control of a disk-type integrated motor-bearing system," *IEEE/ASME Transactions on Mechatronics*, vol. 7, no. 1, pp. 15–22, 2002.

[62] Sung-Ho Park and Chong-Won Lee, "Lorentz force-type integrated motor-bearing system in dual rotor disk configuration," *IEEE/ASME Transactions on Mechatronics*, vol. 10, no. 6, pp. 618–625, 2005.

[63] W. Geng and Z. Zhang, "Investigation of a new ironless-stator self-bearing axial flux permanent magnet motor," *IEEE Transactions on Magnetics*, vol. 52, no. 7, pp. 1–4, 2016.

[64] M. Sumino and S. Ueno, "Rotation test of a tilt-controlling axial self-bearing motor with superconducting magnetic bearing," *2th Int. Conference on Motion and Vibration Control, Sapporo, Japan*, 2014.

[65] S. Ueno, R. Iseki, and C. Jiang, "Stability of a tilt-controlling axial gap self-bearing motor with single-stator," *Mechanical Engineering Journal*, vol. 4, no. 4, pp. 16–00 337–16–00 337, 2017.

[66] S. Ueno, K. Nakazawa, and C. Jiang, "Improvement of stability of an tilt-controlling axial gap self-bearing motor with single stator*," in *2019 12th Asian Control Conference (ASCC)*, 2019, pp. 1216–1221.

[67] S. Ueno, T. Fukuura, and T. Van Toan, "A 5-dof active controlled disk type pm motor with cylindrical flux paths," in *14th International Symposium on Magnetic Bearings*, 2014.

[68] C. Jiang, K. Adnou, and S. Ueno, "5-degree of freedom active position control of an axial self-bearing motor with six concentrated stator windings," in *15th Int. Symposium on Magnetic Bearings*, 2016.

[69] M. Osa, T. Masuzawa, and E. Tatsumi, "5-dof control double stator motor for paediatric ventricular assist device," in *13th International Symposium on Magnetic Bearings*, 2012.

[70] M. Osa, T. Masuzawa, N. Omori, and E. Tatsumi, "Radial position active control of double stator axial gap self-bearing motor for paediatric vad," in *14th International Symposium on Magnetic Bearings*, 2014.

[71] N. Kurita, T. Ishikawa, N. Saito, T. Masuzawa, and D. L. Timms, "A double-sided stator type axial bearingless motor development for total artificial heart," *IEEE Transactions on Industry Applications*, vol. 55, no. 2, pp. 1516–1523, 2019.

[72] H. K. Asper and S. Siposs, *Passive Magnetic bearing with integrated motor generator for flywheel applications*. Dresden, Germany: 8th Int. Symposium On Magnetic Suspension Technology, 2005.

[73] J. Van Verdeghem, V. Kluyskens, and B. Dehez, "Dynamical modeling of passively levitated electrodynamic self-bearing machines," *IEEE Trans. on Ind. App.*, vol. 55, no. 2, pp. 1447–1460, March 2019.

[74] J. Van Verdeghem and B. Dehez, "Fully passively levitated self-bearing machines with combined windings," in *2020 IEEE Energy Conversion Congress and Exposition (ECCE)*, 2020, pp. 254–261.

[75] A. Jack, B. Mecrow, and C. Maddison, "Combined radial and axial permanent magnet motors using soft magnetic composites," in *1999. Ninth International Conference on Electrical Machines and Drives (Conf. Publ. No. 468)*, 1999, pp. 25–29.

[76] H. Won, Y.-K. Hong, M. Choi, H.-s. Yoon, S. Li, and T. Haskew, "Novel efficiency-shifting radial-axial hybrid interior permanent magnet sychronous motor for electric vehicle," in *2020 IEEE Energy Conversion Congress and Exposition (ECCE)*, 2020, pp. 47–52.

[77] J. M. Seo, J.-S. Ro, S.-H. Rhyu, I.-S. Jung, and H.-K. Jung, "Novel hybrid radial and axial flux permanent-magnet machine using integrated windings for high-power density," *IEEE Transactions on Magnetics*, vol. 51, no. 3, pp. 1–4, 2015.

[78] L. Zhou, F. Guo, H. Wang, and B. Wang, "High-torque direct-drive machine with combined axial- and radial-flux out-runner vernier permanent magnet motor," in *2021 IEEE International Electric Machine Design Conference (IEMDC)*, 2021, pp. 1–8.

[79] R. N. Zarandi, M. Mirsalim, and A. Tenconi, "A novel hybrid hysteresis motor with combined radial and axial flux rotors," *IEEE Transactions on Industrial Electronics*, vol. 63, no. 3, pp. 1684–1693, 2016.

[80] Z. Q. Zhu, H. Y. Li, R. Deodhar, A. Pride, and T. Sasaki, "Recent developments and comparative study of magnetically geared machines," *CES Transactions on Electrical Machines and Systems*, vol. 2, no. 1, pp. 13–22, 2018.

[81] F. Wu and A. El-Refaie, "Permanent magnet vernier machine: a review," *IET Electric Power Applications*, vol. 13, no. 2, pp. 127–137, 2019.

[82] M. G. Kesgin, P. Han, N. Taran, and D. M. Ionel, "Optimal study of a high specific torque vernier-type axial-flux pm machine with two different stators and a single winding," in *2020 IEEE Energy Conversion Congress and Exposition (ECCE)*, 2020, pp. 4064–4067.

[83] R. Zhang, J. Li, R. Qu, and D. Li, "Analysis and design of triple-rotor axial-flux spoke-array vernier permanent magnet machines," *IEEE Transactions on Industry Applications*, vol. 54, no. 1, pp. 244–253, 2018.

[84] M. Johnson, M. C. Gardner, and H. A. Toliyat, "Design and analysis of an axial flux magnetically geared generator," *IEEE Transactions on Industry Applications*, vol. 53, no. 1, pp. 97–105, 2017.

[85] M. F. H. Khatab, Z. Q. Zhu, H. Y. Li, and Y. Liu, "Comparative study of novel axial flux magnetically geared and conventional axial flux permanent magnet machines," *CES Transactions on Electrical Machines and Systems*, vol. 2, no. 4, pp. 392–398, 2018.